ACTIVE AND PASSIVE SEISMIC SURFACE WAVE METHODS FOR LEVEE ASSESSMENT IN THE SACRAMENTO-SAN JOAQUIN DELTA, CALIFORNIA, USA

Mitchell S. Craig[1]

Koichi Hayashi[2]

Özgür Kozacı[3]

1. Corresponding author:

Department of Earth and Environmental Sciences

California State University, East Bay

25800 Carlos Bee Blvd.

Hayward, CA 94542 USA

mitchell.craig@csueastbay.edu

2. Geometrics, Inc.

San Jose, CA USA

khayashi@geometrics.com

3. InfraTerra, Inc.

San Francisco, CA USA

okozaci@infraterra.com

This article has been accepted for publication and undergone full peer review but has not been through the copyediting, typesetting, pagination and proofreading process, which may lead to differences between this version and the Version of Record. Please cite this article as doi: 10.1002/nsg.12144.

Key words: Seismic, Velocity, Surface wave.

Abstract

Seismic surveys were performed using a novel application of combined active and passive surface wave methods to evaluate the integrity of levees protecting islands in the Sacramento-San Joaquin Delta, California, USA, from flooding. Delta islands have been undergoing rapid subsidence during the past century due to farming practices that have led to the loss of a surficial peat layer. A large earthquake on any one of several active faults in the region could cause multiple levee failures and extensive flooding in the Delta.

Surface wave surveys were carried out along the crest of levees using the active method (2D MASW) and along the base of levees using the passive method (Microtremor Array Method or MAM). 2D seismic S-wave velocity (V_S) profiles were prepared for each site by combining shallow data from the active survey along the crown of the levee with deeper data from a passive survey along the toe of the levee. V_S profiles reveal a low-velocity peat layer beneath the levee body that was confirmed by geotechnical borehole logs. Lateral variability of the levee was evaluated using average velocity to the base of the levee versus along-levee distance.

Keywords: seismic, MASW, S-wave, velocity, geotechnical.

Acknowledgements

This work was funded by the California Energy Commission. Bobby Savoy, Maiyah Matsumura, Stephanie Anderson, and Pratiksha Pandit assisted with data collection despite temperatures over 100°F (38°C). Steve Sinnock facilitated site access and provided access to data. Scott Brandenberg, Yang Yang, Roland Bürgmann, and Xie Hu aided in site selection and the design of velocity models. Comments by Horacio Ferriz and an anonymous reviewer helped to improve the quality of the paper.

Introduction

Earthen levees, sea walls, and dams are used globally for flood protection, water delivery, and water storage. Extreme weather events that lead to high water levels in rivers may result in the failure of levees and dams and catastrophic flooding. Earthquakes may also trigger the failure of levees and dams. Coastal areas will experience higher water levels in the coming decades due to sea level rise, and levees will require increased maintenance. Near surface geophysical methods are essential tools for assessing the integrity of earthen levees and dams. Seismic surface wave methods were used in conjunction with electrical resistivity methods to evaluate a levee in the Mississippi River Valley (Rahimi et al., 2018). Geotechnical borehole data were used to investigate the relationship between seismic velocity, electrical resistivity, and soil type in Japanese levees (Hayashi et al., 2013, 2019). Ambient noise tomography was used to investigate levees in New Orleans that failed in 2005 due to the storm surge of Hurricane Katrina (Hayashi et al., 2018). Ambient noise was also used to measure temporal variations in seismic velocity of the Colijnsplaat sea levee in the Netherlands due to tidal fluctuations (Planès et al., 2017).

The Sacramento-San Joaquin Delta (the Delta), is part of the San Francisco Estuary in California and is subject to tidal influence (mean range approximately 1 m) from the Pacific Ocean. Sandy alluvial fan deposits of the Pleistocene are overlain by a Holocene peat and mud up to 10 m thick (Atwater and Belknap, 1980). The Delta is an exceptionally productive agricultural region and the site of key elements of the water and energy infrastructure of the state (Wolff, 2003). The Delta has undergone 3 to 8 m (10 to 25 ft) of subsidence following the construction of levees and drainage systems, which led to significant loss of peat (Ingebritsen and Ikehara, 1999).

Subsidence of Delta islands has increased their risk of flooding due to levee failure (Mount and Twiss, 2004). Deposits of peat and mud several meters thick throughout the Delta present engineering challenges for the construction and maintenance of water and energy infrastructure. The response of a levee to earthquake shaking or pressure from a river is related to the strength of its materials. Seismic S-wave velocity, $V_S = \sqrt{\mu / \rho}$, (μ = small strain shear modulus and ρ = density) is commonly used as a proxy for the strength of geologic materials. Average S-wave velocity to a specific depth is widely used in engineering seismology for UBC site classification, commonly to depth of 30 m (V_{S30}) (Building Seismic Safety Council, 2001). Maps of V_{S30}, (average V_S to a depth of 30 m) have been prepared for California for earthquake hazard site assessment (Wills and Clahan, 2006; Wills et al., 2015).

Seismic velocity normally increases with depth, because geologic materials become stronger with depth due to increased pressure; older sediments are better compacted and better cemented. One of the underlying assumptions of the seismic refraction method, widely used in near surface studies, is that velocity increases with depth. Downgoing raypaths in a layered medium that monotonically increases in velocity with depth will be refracted away from the normal at each interface, until they are critically refracted and start to return to the surface as head waves. However, at an interface where velocity *decreases* with depth (a velocity reversal), the refraction method will fail to detect the interface (Reynolds, 2011).

Velocity reversals sometimes occur in coastal areas where engineered fill is placed on top of softer sediments. In the Delta in general, and on McDonald Island in particular, levee fill tends to have a higher velocity than the underlying peat and mud. Hence the traditional seismic refraction method is unable to provide key details needed to model levees and their underlying materials. Seismic surface wave methods, on the other hand, are able to detect velocity reversals.

Combined active and passive seismic surface wave methods provide a suitable tool for measuring shear wave velocity, especially in areas where levees are underlain by soft peat. In general, the active surface wave method using a land streamer and impulsive source may obtain sufficient depth penetration to measure the velocities of levee fill material and underlying peat; however it may not be able to reach the stiffer material underlying the peat. By recording a separate passive survey at the base of the levee, it may be possible to obtain the additional depth penetration needed to measure the velocity of the deeper stiff unit underlying the peat.

In this study, seismic surveys were conducted at three sites on McDonald Island (Figure 1) in order to measure V_S and evaluate the suitability of the method for assessing the condition of the levee. Sites were selected to represent a range of geologic and engineering conditions after review of topographic maps, soil maps, aerial photographs, and based on the availability of geotechnical borehole logs. Site 1 is at the north end of the island where a tidal channel, Whiskey Slough, intersects the levee. Site 2 is at the south end of the island, where the levee is believed to be undergoing subsidence at a relatively high rate, and Site 3 is on the northeast side of the island, in an area thought to be relatively stable.

Historic topographic maps from the USGS 7.5' quadrangle series were reviewed for information on modifications to the island and the rate of subsidence. Four quadrangles intersect on McDonald Island at 38°00' N, 121°30' W. The 1910 Headreach (now Terminous) quad shows the northern portion of McDonald Island as undeveloped tidal marsh, with no evidence of alterations to meandering tidal channels, including the northern end of Whiskey Slough. We thus assume the elevation of McDonald Island to be zero in 1910. The 1913 Holt quad shows the southeast corner of McDonald Island as unrestricted marsh, however Empire Cut, a linear and evidently manmade feature that forms the southern edge of McDonald Island, is present. There is presumably some sort of levee along the edge of this cut, which is discussed further below. By 1952, the island surface appears to have fallen 5 to 10 ft (1.5 to 3 m). By 1978, it had dropped an additional 5 ft (1.5 m), to an elevation of -10 to -15 ft (-3 to -4.5 m) relative to MLLW (mean lower low water). Numeric quantities in this paper are generally listed first in native units, Imperial or SI, followed by the SI equivalent if needed.

A drilling program was carried out on McDonald Island in 1958 consisting of 34 boreholes with 1000 ft (328 m) spacing, covering about 75% of the perimeter of the island, including two of the three sites where we conducted seismic surveys for this study (California Department of Water Resources, 1958). Boreholes were 1-inch (2.5 cm) diameter. Graphic logs of soil type versus depth were prepared based on visual classification. Standard penetration testing (SPT) was performed using a 100-lb (45 kg) hammer. The thickness of peat varied from about 5 to 15 ft (1.5 to 5 m) and the depth to the top of the stiff layer as identified by SPT testing was about 15 to 25 ft (5 to 7.5 m).

Peat thickness was measured throughout the Delta using hand auger boreholes in a comprehensive study covering twenty 7.5 minute quadrangles, including McDonald Island, and the results were used to prepare stratigraphic cross sections across the Delta (Atwater and Belknap, 1980; Atwater, 1982). An updated map of the thickness of the peat layer in the Delta incorporating 900+ geotechnical borehole logs shows that peat varies from zero to 9 meters in the central Delta, with most areas having intermediate values of about 4-5 meters (Unruh et al., 2016).

Borehole logs from 2004 and 2011 were available for two of the sites on McDonald Island where we conducted seismic surveys. These include Unified Soil Classification (USC) soil types and standard penetration test (SPT) data.

Methods

Seismic Surface Wave Method

Seismic surface wave methods were used to determine S-wave velocity (V_S) of the levee body and underlying material. Surface waves differ fundamentally from body waves in that they are dispersive, meaning that different wavelengths travel at different velocities. The property of dispersion may be exploited to determine velocity versus depth. For an overview of surface wave methods, see Reynolds (2011, p. 208-215). For an explanation of how surface waves are generated in elastic media, see Bullen and Bolt (1985). Combined active and passive methods were used for the determination of one dimensional (1D) velocity depth profiles for site characterization in the San Francisco Bay area by Craig and Hayashi (2016). In the present study, 2D velocity depth profiles were obtained.

Data Acquisition

2D profiles were acquired with an orientation parallel to the levee. Line length ranged from about 200 to 300 m at the three sites. At each site, a pair of parallel lines was recorded, one along the crest (crown) of the levee and the other along the base (toe) of the levee, with a spacing of about 30 m between the lines. Surveys were carried out at the three sites using identical equipment and recording parameters.

Active Method

An active seismic method, multichannel analysis of surface waves (MASW: Park et al., 1999; Xia et al., 1999; Ivanov et al., 2006) was used along the crest of the levee. Active surveys were conducted using a 24-channel seismograph (Geometrics Geode), land streamer with 4.5 Hz geophones spaced 2 m apart, providing a 46-meter spread length. A sledgehammer source was used, with an 8 m moveout between shots.

Sample interval was 4 ms and record length was 4.096 seconds. Surveys were carried out using a moving spread with end-on geometry.

Passive Method

A passive method, the microtremor array method (MAM: Aki, 1957; Louie, 2001; Okada, 2003) was used along the levee base. Passive surveys were performed along the base of the levee using cableless seismographs (Geometrics Atom), each with a 2 Hz geophone, to record ambient noise. A total of 30 seismograph units was used, with a receiver spacing of 5 m, providing a spread length of 145 m. Sample interval was 4 ms. The record length was 30-60 minutes for each patch. The spread was rolled 2-3 times, each time with 50% overlap, providing total survey lengths of 200 m at Site 3 and 300 m at Sites 1 and 2.

Data Processing

Seismic waveform data was used to determine a one-dimensional (1D) velocity depth profile at each location along the levee, and the 1D profiles were combined to produce a two-dimensional (2D) profile. Data were processed using SeisImager/SW software (Geometrics, 2009). Active and passive data were processed separately through the preparation of frequency-velocity spectra and the picking of dispersion curves. Active data were processed using the common midpoint cross correlation (CMP-CC) method (Hayashi and Suzuki, 2004). Passive data were processed using the common midpoint spatial autocorrelation (CMP-SPAC) method (Hayashi et al., 2015).

Both active and passive data were first sorted into common midpoint (CMP) gathers using a 10 m bin size. Active and passive data from each location were processed to produce a combined dispersion curve and 1D velocity-depth profile. An example of data analysis performed for one CMP (Site 1, distance 110 m) using active and passive methods is described below.

In active surveys, each CMP gather (Figure 2a) was transformed from the time-distance domain to the frequency-velocity (f-v) domain (Figure 2b) using a phase shift and stack method (Park, 1999). Passive data from each CMP were processed using the spatial autocorrelation (SPAC) method to prepare a coherency gather (Figure 3a), which was transformed to the f-v domain (Figure 3b). Active and passive dispersion curves from each location were picked separately, then combined and edited to provide a single dispersion curve (Figure 4) from 2-30 Hz. A nonlinear least-squares inversion was carried out to minimize the RMS error between observed and theoretical dispersion curves, including higher modes up to the 10^{th} mode (Figure 5), see Hayashi and Craig (2017). Dispersion curves from the active surveys contained an appreciable amount of higher modes (Figure 5a). A genetic algorithm (GA) inversion of the same data is provided as an example (Figure 5b). The GA inversion provides lower error but requires much longer computation times and was not used for 2D processing. By including passive data, dispersion curves may be extended to lower frequencies, which allow velocities to be estimated at greater depths (Figure 5c).

At each CMP location, dispersion curve picks were used to construct an initial 1D velocity model by mapping each pick to a depth equal to one-third its wavelength (e.g., Gazetas, 1982). As an example of the depth range of the active and passive methods, velocity models based on the dispersion curves above were prepared based solely on active data (Figure 6a) and combined active and passive data (Figure 6b). Additionally, a genetic algorithm inversion was performed on the active data and provides additional information on the uncertainty of velocity estimates (Figure 6c).

Velocity models were 15 m deep and consisted of 15 layers ranging from 0.5 m thick at the surface to 1.5 m thick at the bottom of the model, with a linear increase in thickness with depth. The range of velocities allowed in the inversion was determined for each of the three 2D lines based on the range of velocities in the dispersion curve picks. Minimum velocities were 72-77 m/s and maximum velocities were 301-450 m/s. As explained above, active and passive data from each CMP location were used to prepare a dispersion curve and 1D velocity model, then the 1D models were concatenated to produce a 2D velocity profile.

Geometry assignment and positioning

Distance posts are maintained along the levee road at a 1000 foot (328 m) spacing by the California Department of Water Resources (DWR). For seismic data acquisition and processing, a local coordinate system was established based on shot and geophone positions and tied to DWR distance posts. A 2D coordinate system was used, with distance along the levee and depth from the recording surface as the coordinates. The counter-clockwise direction along the levee road was taken as the positive direction for distance. The data processing grid and velocity model grid points were established based on shot and geophone locations. For the active (MASW) surveys, geophone spacing was 2 m and the common midpoint (CMP) bin size used for data processing was 10 m. For passive surveys, geophone spacing was 5 m and the CMP bin size was 10 m.

For passive surveys, position was determined from an internal GPS in each seismograph unit. Active seismic surveys were conducted along the levee crown road, and position of the active survey relative to distance posts was determined with measuring tape. Some redundant positioning data was obtained by using a handheld GPS receiver to collect selected shotpoint and geophone locations for the active survey, along with the nearest DWR distance posts.

Active and passive lines were recorded on the same day at each site and were laid out parallel to each other with their ends aligned.

Results

Results are presented by site. The main data product for each site is a 2D seismic S-wave velocity (V_S) section prepared by combining data from active and passive surveys. Velocity models 15 m deep were prepared in order to capture near-surface details of the velocity model important for characterizing the levee and the materials immediately beneath it. A basemap is provided for each site showing the location of seismic lines and borehole logs. A borehole log is compared with the velocity section for each site. A basic interpretation of each seismic profile is provided here, with additional comments in the Discussion section.

Site 1 – North

Site 1 is located at the north end of the island, where Whiskey Slough intersects the north edge of the island at Columbia Cut (Figure 1). A pair of seismic lines 300 m long were positioned to cross the projected paleochannel of the slough (Figure 5). One line was recorded along the crest of the levee using the active (MASW) method and other was recorded along the levee base using the passive (MAM) method. Seismic lines were oriented perpendicular to the channel axis. Data from the two methods were combined as described above to prepare a 2D seismic profile (Figure 6). The projected channel of the slough is located in the center of the seismic profile.

Velocities near the surface (upper 2 m) are ~150 to 200 m/s (green), and correspond to relatively stiff levee fill material. Velocities decreases rapidly with depth over the depth range 2 to 4 m (yellow), and reach a minimum value of about 90-100 m/s (orange) at most locations. These low velocities correspond to softer organic clay and peat beneath the levee.

Borehole 1-B2 (ENGEO, 2011) drilled on the crest of the levee at this site, shows levee fill material 3.2 m thick, underlain by clay. Two boreholes from the 1958 transect described above (Calif. DWR, 1958, Boreholes 23 and 24) nearly coincide with the ends of the seismic profile at the base of the levee at this site. They indicate a soft layer of peat and organic clay ~7.6 m (25 ft) thick over a stiff layer.

Site 2 – South

Site 2 is located along the southern edge of the island along Empire Cut (Figure 1). Again, a pair of parallel seismic lines was recorded, one along the levee crest using the active method, and the other along the levee base using the passive method (Figure 8a). As before, data from the two surveys were combined to produce a 2D S-wave velocity (V_S) section (Figure 8b). Velocities at the surface are 140-150 m/s (yellow), decreasing with depth until reaching a minimum of ~80-100 m/s (orange) at a depth of 4-6 m. The low-velocity zone here is thinner and more laterally continuous than the one at Site 1.

Borehole EB-1 (Lowney Associates, 2004), drilled on the crest of the levee, encounters ~3 m of levee fill material, followed by a section of peat with an extraordinary thickness of 7 m, before reaching a stiff layer (ML) at ~10 m depth. Soil type at 13.5 m is SP-SM (poorly graded sand with silt), and at 16.7 m depth is SP (poorly graded sand).

Site 3 – East

At Site 3, located on the eastern side of the island next to the San Joaquin River (Figure 1), a pair of parallel 300 m long seismic profiles, one along the levee crown and one along the levee toe, was recorded along a curved section of the levee between distance posts 150+00 and 140+00 (Figure 9a). Acquisition using the towed landstreamer along a curved path required the constant attention of field personnel to maintain its position along the shoulder of the road.

The velocity profile at this site (Figure 9b) shows a low-velocity zone at a depth of 4-6 m, with V_S of 70 to 100 m/s (red and orange colors). The low velocity zone appears to either pinch out to the southeast or be truncated laterally at a distance of ~200 m.

A log from soil borehole 58-4 (Calif. DWR, 1958), located near the midpoint of the seismic profile but on the land side, is a graphical log from a transect showing a laterally continuous peat layer that is 3.6 m thick at this location, underlain by silt and clay.

Average velocity

In order to characterize lateral variations in seismic shear wave velocity (V_S) of the levee body along the length of the levee, the average velocity to a specific depth may be used. While average velocity is commonly calculated to a depth of 30 m for UBC site classification (V_{S30}), it may be calculated to any arbitrary depth z, (V_{Sz}). In this work, average velocity was calculated to a depth of 3 m in order to characterize the average velocity of the levee body. A depth of 3 m was chosen as that is the approximate thickness of levee fill based on borehole logs. Average velocity V_{S3} versus distance along the levee was accordingly produced for each of the three sites, consisting of average V_S to a depth of 3 m (Figure 10).

Discussion

A measure of the accuracy of velocity estimates is provided by the RMS error (RMSE) between the theoretical and observed dispersion curves (Figure 5). Dispersion curves were picked automatically from f-v spectra and edited as needed. Dispersion curve picks used for inversion were limited to the band 2-30 Hz. RMSE was calculated for each analysis location. In general, f-v spectra that contain primarily fundamental mode energy with clear, unambiguous dispersion curves will have the scatter in picks and small RMSE. Spectra that are noisy or that have dispersion curves with strong higher modes are more difficult to pick and will have higher RMSE. In this study, an RMSE of 10-15 m/s indicates good data quality, RMSE of 15-20 is acceptable quality, and data with RMSE greater than 20 should be checked and dispersion curve picks edited if needed.

Average RMSE and percent error for the three sites were as follows: Site 1: RMSE = 18.8 m/s, 16.2%; Site 2: RMSE = 19.0 m/s, 13.6%; Site 3: RMSE = 32.2 m/s, 21.0 %. Percent error is calculated point by point for each dispersion curve, then the percent values are averaged for the site. The average RMSEs for Sites 1 and 2 are similar to each other and to the RMSE of the example analysis, 20.0 m/s (Figure 5c). The average RMSE of Site 3 is somewhat higher and review of its dispersion curves (not shown) reveals higher scatter of dispersion curve picks and some frequency ranges with missing picks. We experienced difficulties with data acquisition during the active survey at this site. While towing the land streamer along a curved gravel road on the crest of the levee we did experience some problems with sensors tipping over and not being noticed for a few shots, which could explain higher noise levels and missing picks.

While the RMSE does provide a numeric indication of goodness of fit, it can be counterproductive to place too much emphasis on it rather than the information content of the data. E.g., the RMS error for the least-squares inversion of the active data alone (Figure 5a) is fairly low at 7.8 m/s, while the inversion that includes both active and passive data (Figure 5c) has much a higher RMS error of 20.0 m/s. Does this mean that we shouldn't use the passive data? We can more fully evaluate the results from these two inversions by comparing the velocity model based on the active method (Figure 6a) with the velocity model based on both active and passive data (Figure 6b). At depths below 8 m, the passive method contributes nearly all of the dispersion curve picks, and is the primary source of velocity information, so we should definitely include the passive data, even though it may cause a higher RMSE.

The vertical resolution of the seismic surface wave method is limited by the minimum wavelength detected and recorded, which depends on the geophone spacing as well as the source signal and geologic properties. The vertical resolution in this study is estimated to be 1-2 m near the surface. Frequency-velocity spectra and dispersion curves were only shown to a maximum of 30 Hz in the examples above, and dispersion curves generally contained higher modes only up to the 3rd or 4th mode. The horizontal resolution is the highest in the upper few meters of the velocity models, including the levee body. This portion of the velocity model is derived from the active survey. Horizontal resolution is controlled by the CMP bin size, 10 m. Different geophone spacings were used for data acquisition in active and passive surveys; a 2 m spacing was used for active surveys and 5 m for passive. The same CMP bin size (10 m) was used for both surveys, making it possible to utilize all data from the two methods.

The active surveys, conducted along the crest of the levee, provided the primary velocity information for the upper ~5 m, including the ~3 m thick levee body and ~2 m of the lower-velocity material immediately beneath. The passive survey contributed velocity information for the material beneath the levee, and was the primary source of velocity information at depths below ~8 m, as explained above. The depth penetration of active surveys was limited due to the low velocity of the material and the presence of strong higher modes. Passive surveys, conducted at the base of the levee, provided dispersion curves that could be picked to frequencies as low as ~1.7 Hz, corresponding to depths of ~60-80 m.

Borehole logs from Site 2 (South) and Site 3 (East) indicate the presence of a peat layer at or near the surface, which is consistent with observations from other islands in the Delta. At Site 1 (North), borehole log 1-B2 (Figure 7a) indicates the presence of fat clay (CH) beneath the levee fill, however some organic material is noted. This borehole log was incomplete, only 7.5 m (25 ft) was available out of a total depth of 12 m (41 ft).

The velocity profile from Site 1 (Figure 7b) shows significant lateral variations in velocity for two different depth ranges that appear to be unrelated. Lateral velocity variations in the depth range from the surface to 3 m are due to variations in the levee fill materials and are captured by V_{S3} , the average velocity to 3 m depth (Figure 10), described below.

Lateral variations in velocity in the levee body, along the length of the levee, were compared by examining V_{S3}, average velocity over the upper 3 m. The average velocity at Site 1 (North) is clearly higher than at the other two sites. There are also stronger lateral variations in velocity at Site 1 than at the other sites, its profile has the shape of cats ears, symmetric about the channel axis of Whiskey Slough. The V_{S3} versus distance profiles for Sites 2 and 3 appear similar, both are fairly constant, with V_S generally 130-150 m/s. Velocities at Site 1 are markedly higher, at 150-210 m/s, indicating stiffer levee fill. Velocities at Site 1 are also much more variable, exhibiting rapid swings, which indicate changes in the stiffness of the levee fill materials over short distances.

Lateral variations in velocity also occur across the lower portion of the velocity profile for Site 1 (Figure 7), at depths from 4 to 10 m. In the center of this profile, where it crosses the apparent paleochannel of Whiskey Slough, V_S is considerably higher than on either side. The higher velocities may correspond to coarser-grained (sandier) sediments than surrounding areas. At these depths, sandy sediments can be stiffer and have higher V_S than peat or soft clay.

At Site 2, Empire Cut (Figure 8), the low velocity zone at a depth of 4 m evidently corresponds to the top of the peat layer beneath the levee body. Borehole EB-1 (Lowney Associates, 2004) was one of four holes at the site, two drilled on the crest of the levee and two on the land side. The boreholes on the crest show that the peat directly underneath the levee is an exceptional ~7 m thick, while the holes on the land side of the levee (off of the levee) only penetrated 1-3 m of peat. The greater thickness of peat underneath the levee may be a relict of the construction technique, the original levee may have been constructed from peat. Empire Cut, on the water side of this levee, has existed since at least 1911, so the original levee must be at least that old.

The 1958 borehole logs provide valuable information on the lateral extent and continuity of stratigraphic units around most of the island. However, these boreholes were not drilled on the crest of the levee, and due to ongoing subsidence and loss of peat, the elevation datum and peat thickness shown in the logs may have changed.

At Site 3, borehole 58-4 (Calif. DWR, 1958) was drilled on the land side of the levee, and does not show any levee fill material at the top of the log. We assumed that the top of this log lies at a depth of about 3 m relative to the crest of the levee (3 m is the thickness of levee fill encountered in boreholes at the other two sites).

The thicknesses of the levee fill materials from borehole logs at Sites 1 and 2 are in reasonable agreement, at 3.2 and 2.9 m. Average velocity to a depth of 3 m versus along-levee distance provides a useful 1D summary product for characterizing overall levee resilience or fragility.

Conclusions

Seismic surface wave methods are well-suited for evaluating levees constructed on top of peat in part because of their ability to detect velocity reversals. Velocity reversals commonly occur where levee fill material overlies peat. A low-velocity peat layer was detected at all three sites in this study, and was confirmed by soil borehole logs.

Combined active and passive seismic surface wave methods provide a suitable tool for measuring shear wave velocity, especially in areas where levees are underlain by soft peat or clay. In general, the active surface wave method using a land streamer and impulsive source may obtain sufficient depth penetration to measure the velocities of levee fill material and underlying peat; however, it may not be able to reach the stiffer material underlying the peat. By recording a separate passive survey at the base of the levee, we were able to obtain the additional depth penetration needed to measure the velocity of the deeper stiff unit underlying the peat.

The average velocity to a depth of 3 m provides a useful summary data product for characterizing levee strength versus along-levee distance on this island.

Conflict of Interest Statement

The authors have no conflicts of interest to declare.

Data Availability

The data that support the findings of this study are available from the corresponding author upon reasonable request.

Figure Legends

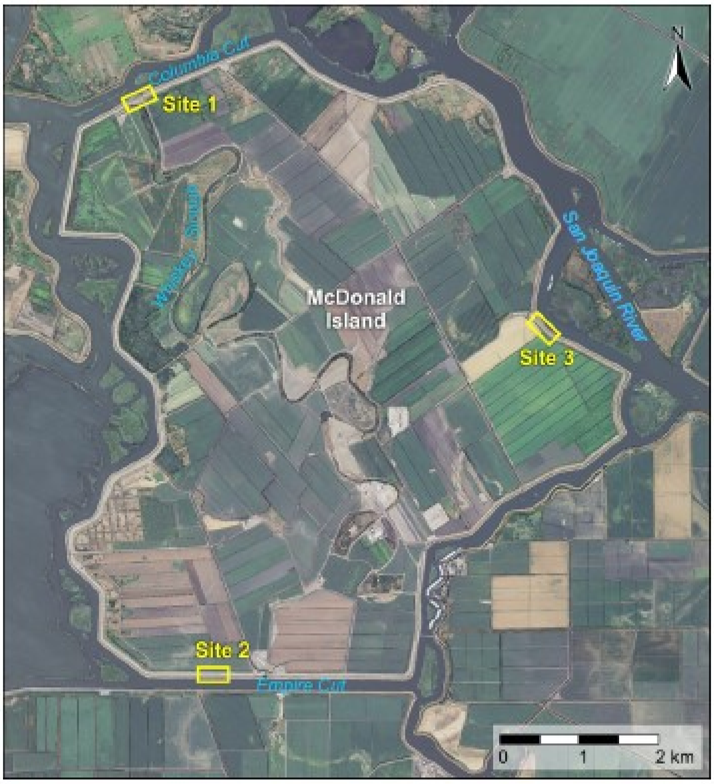

Figure 1. Satellite image of McDonald Island showing three sites where geophysical surveys were performed. Site 1 is located to the north, where Whiskey Slough intersects the edge of McDonald Island at Columbia Cut, Site 2 is located along the southern edge of the island is bounded by Empire Cut, and Site 3 is on the eastern side of the island, next to Spud Island.

a)

b)

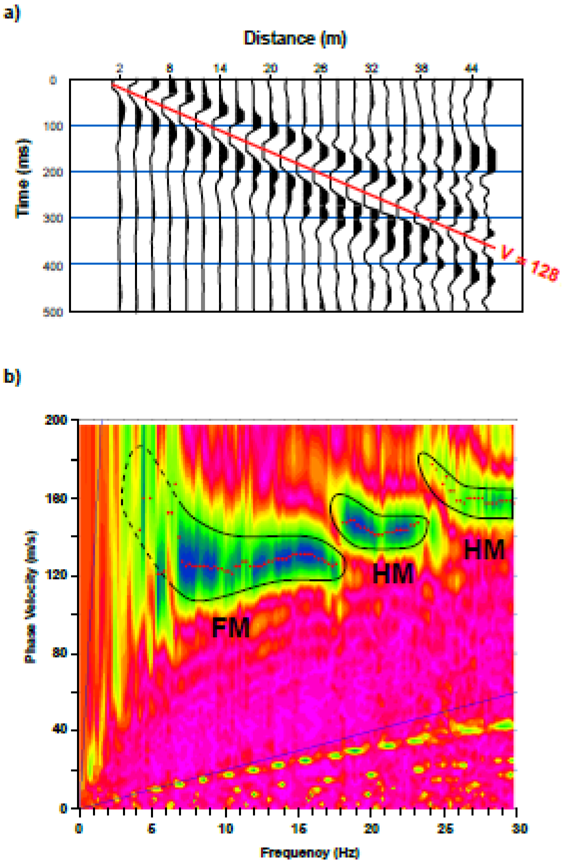

Figure 2. CMP gather and frequency velocity spectra, active method. a) CMP gather. Red line indicates surface wave arrival with phase velocity of 128 m/s. b) Frequency-velocity spectrum from active method, with small red dots indicating dispersion curve autopicks. Both fundamental mode (FM) and higher mode (HM) dispersion curves are present and have been picked. Cool colors (blues and greens) correspond to highest energy. The majority of the picks in the fundamental mode have velocities in the range of 120-130 m/s, in general agreement with the apparent velocity of surface waves in Figure 2a above.

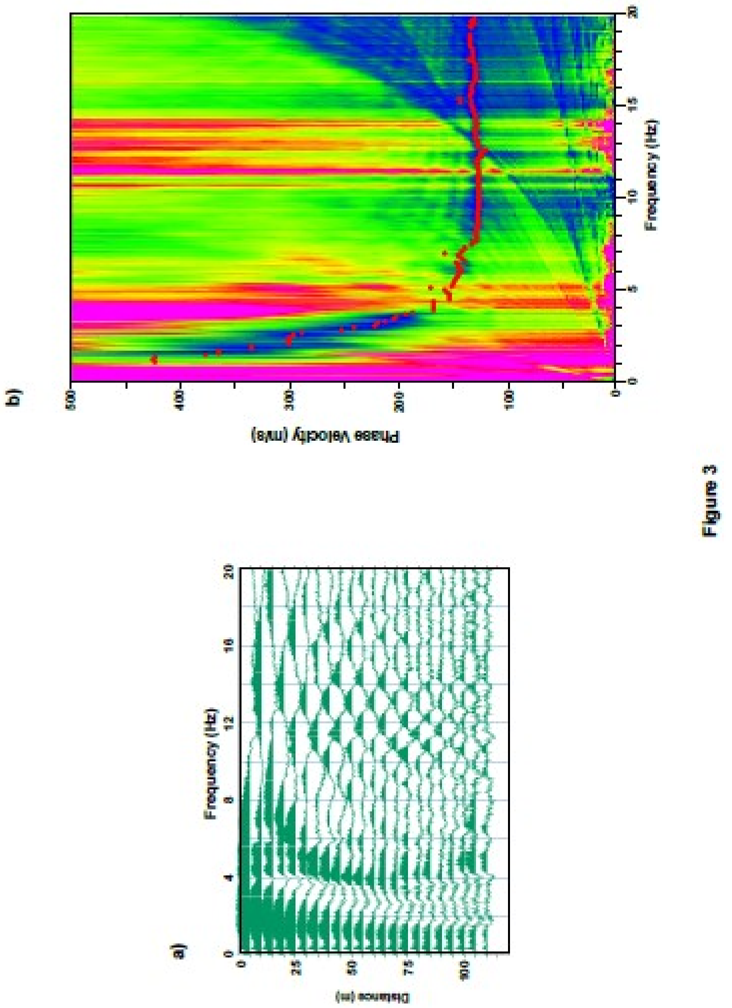

Figure 3. Coherence and frequency-velocity spectrum from passive method. a) Coherence, or cross correlation of seismic traces from two different sensors normalized by power. Distance is sensor separation. b) Frequency-velocity spectrum. Small red dots indicate fundamental mode dispersion curve autopicks along the trajectory of cool colors (blues and greens), which correspond to velocities with the lowest error.

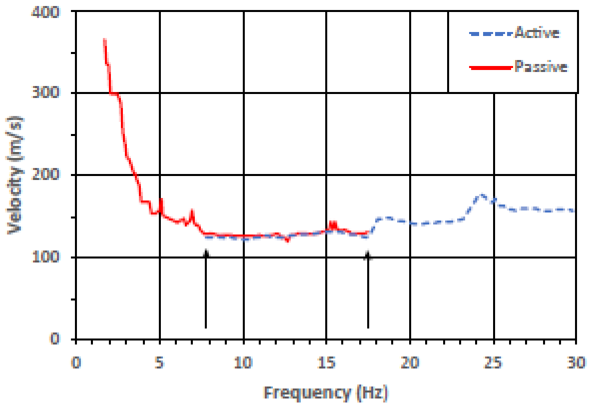

Figure 4. Combined dispersion curves from active and passive methods at the example analysis location. The passive dispersion curve provides velocity estimates from 1.7 Hz to 12.5 Hz, and the active dispersion curve provides usable data from 8 Hz to 30 Hz. The two curves overlap and are in close agreement from 8 to 12.5 Hz.

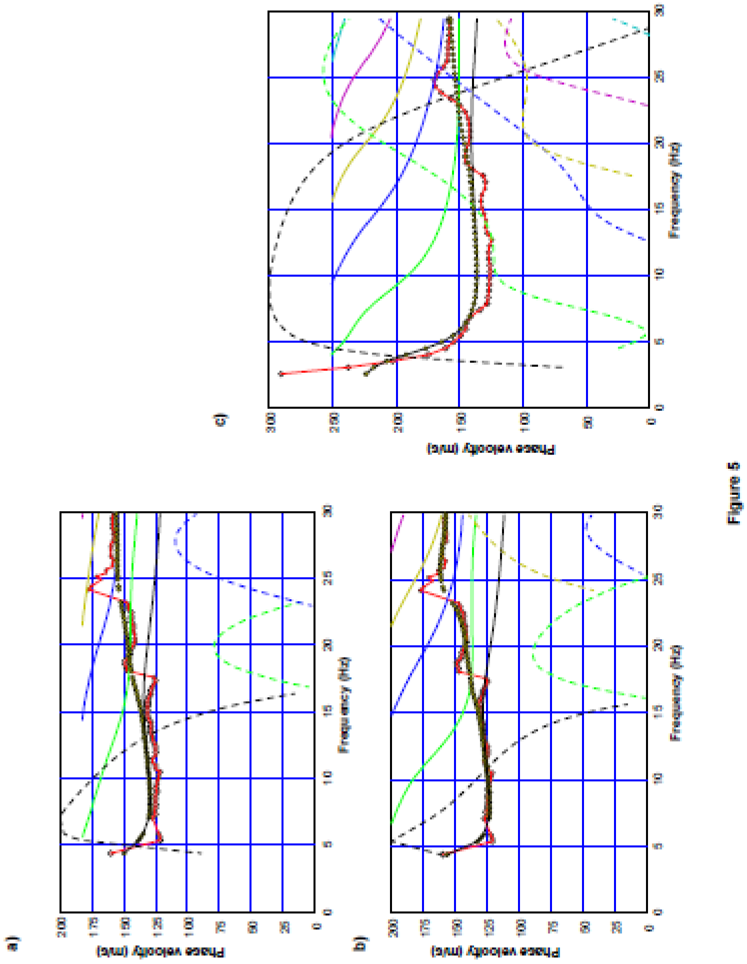

Figure 5. Inversion results from example location (Site 1, CMP 110 m), showing difference between observed and theoretical dispersion curves. a) Active method, least squares method, RMS error 7.8 m/s, b) active method, genetic algorithm, RMS error 5.0 m/s, c) combined active and passive methods, RMS error 20.0 m/s. The theoretical dispersion curve, or effective mode, is a weighted average of the fundamental mode and the first 10 higher modes. Solid red curves and white circles are observed dispersion curves (edited picks from Figures 2b and 3b above). Yellow circles show the effective mode, a weighted average of the theoretical fundamental mode (solid black line) and higher mode dispersion curves (solid

green, blue, etc., lines). The weight of each mode is shown with a dashed line of the same color.

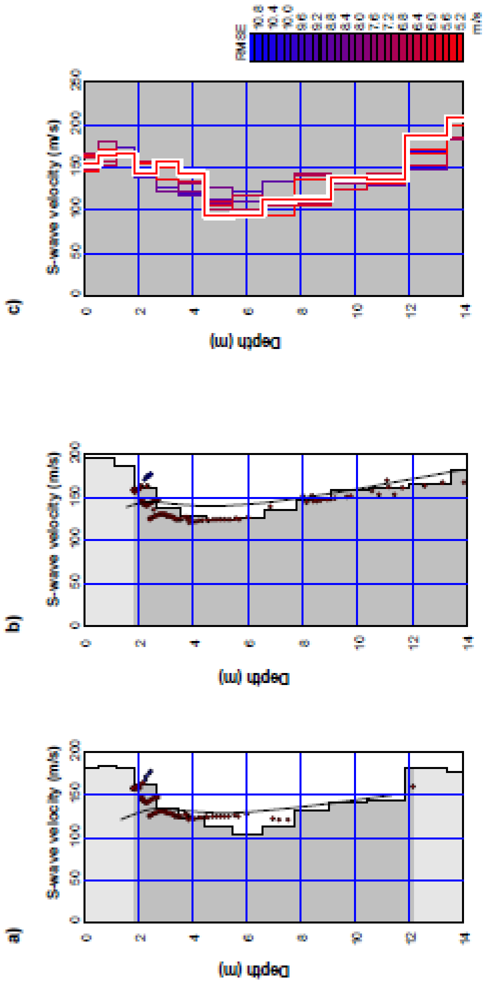

Figure 6

Figure 6. Inverted 1D velocity models from example location, CMP 114. a) Active method, nonlinear least squares inversion. Red dots are dispersion curve velocity picks mapped to depth. Dark grey zone corresponds to depth range supported by picks. Black curve corresponds to fundamental mode dispersion curve. Velocity decreases with depth over the depth range of 2 to 5 m, reaching a minimum of about 100-125 m/s over the depth range of ~5-7 m. These low velocities correspond to soft mud or peat immediately beneath the levee. b) Combined active and passive methods. Velocities at depths greater than 6 m are better

constrained due to additional dispersion curve picks from the passive method. c) Genetic algorithm, based on data from active survey. 50 models with best model highlighted in white. Red to blue color scale indicates RMS error of each model.

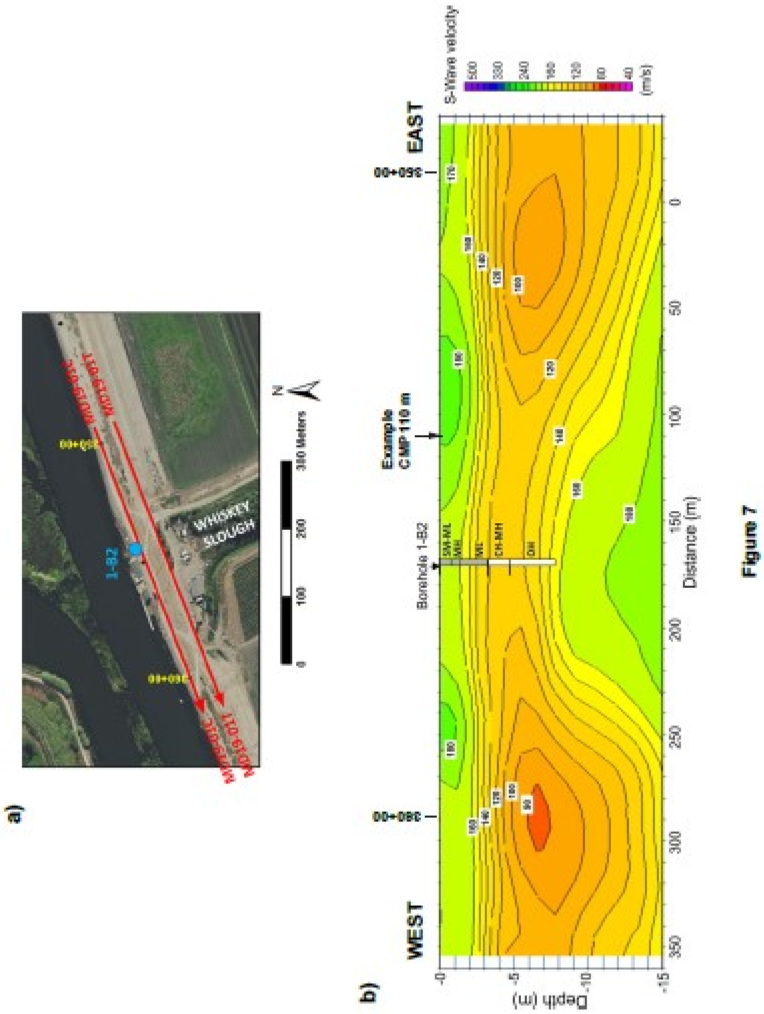

Figure 7. Map and velocity profile, Site 1, northern end of island at Whiskey Slough. a) Map of site. Seismic lines shown in red. Borehole 1-B2 shown with blue circle. Seismic line MD19-01C is on crown of the levee and MD19-01T is along the toe. Yellow numerals are DWR distance posts with 1000 foot (328 m) spacing. b) S-wave velocity (V_S) profile, VE = 5. Distance posts are DWR 1000-foot markers. Data from combined active and passive

surveys. Higher-velocity material in uppermost 3 meters corresponds to levee fill material. Velocity decreases sharply at ~3 m depth. Borehole log 1-B2 at Site 1 (North), drilled in 2011, showing 3.2-m-thick levee fill material (gray section of the borehole) composed of silty sand (SM) and silt with sand (ML), underlain by fat clay/elastic silt (CH-MH), followed by organic clay (OH). See map above (Figure 7a) for borehole location (ENGEO, 2011).

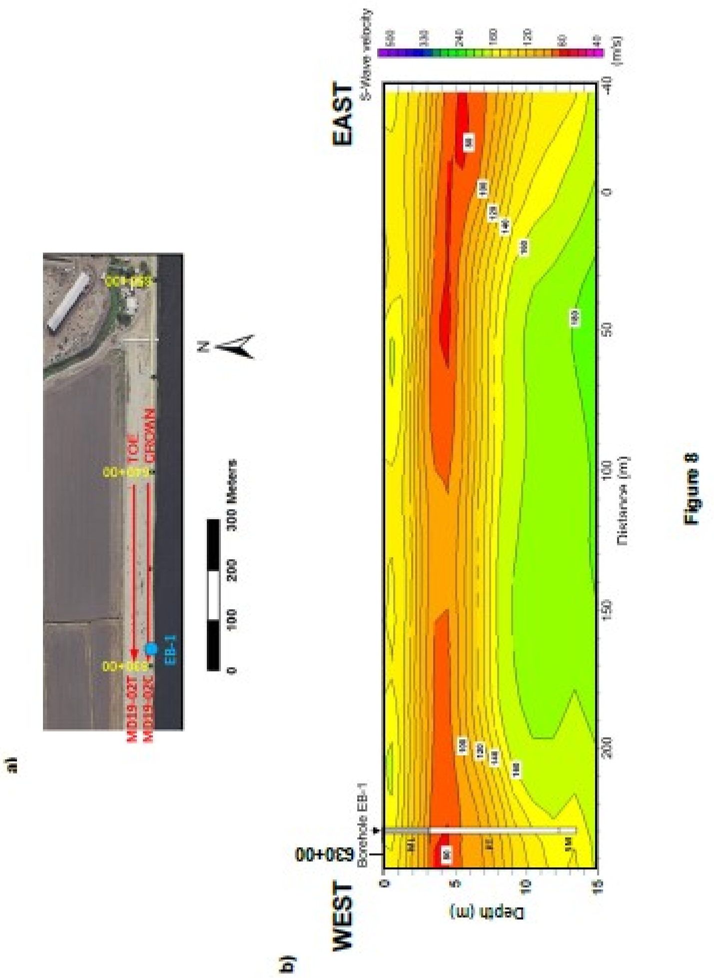

Figure 8. Map and velocity profile, Site 2, southern edge of island at Empire Cut. a) Map of site. Seismic lines (red) were recorded along crown (crest) and toe (base) of levee between distance posts 640+00 and 630+00. Location of borehole EB-1 indicated with blue circle. b) S-wave velocity (V_S) model, VE = 5. Data from combined active and passive surveys.

Borehole log EB-1 drilled in 2004, located at the west end of the profile, distance post 630+50. Levee fill (gray section of the borehole) material is 2.9 m thick and composed of sandy silt (ML). Base of peat (Pt) is at 10.1 m. Peat is underlain by silty sand (SM) (Lowney Associates, 2004).

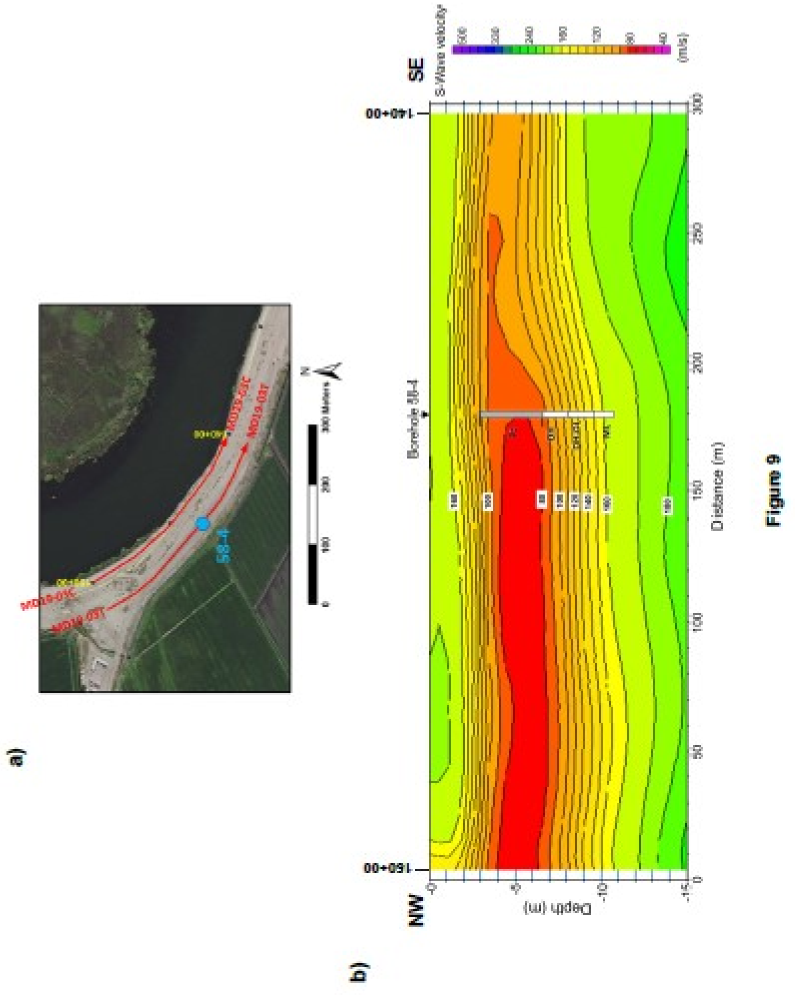

Figure 9. Map and velocity profile, Site 3, eastern side of island. a) Map showing location of seismic profiles (red). Arrow indicates recording direction of active survey. Yellow numerals are DWR 1000-foot distance posts. Borehole 58-4 shown by blue circle. b) S-wave velocity (V_S) profile, VE = 5. Log from soil borehole 58-4 (Calif. DWR, 1958). Region in dark orange

Accepted Article

corresponds to very low velocities of less than 100 m/s that evidently correspond to peat (Pt) beneath the levee body, starting at a depth of ~4 meters.

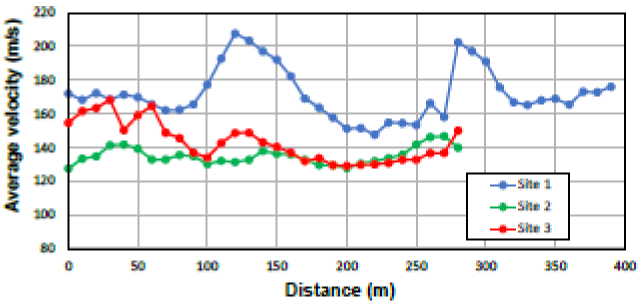

Figure 10

Figure 10. Average S-wave velocity to a depth of 3 meters along levee at each of the three sites. This depth corresponds approximately with the base of the levee. Velocity at Site 1 (North) is notably higher than Sites 2 and 3 and has strong lateral variations.

References

Aki K. 1957. Space and time spectra of stationary stochastic waves, with special reference to microtremors. Bulletin of the Earthquake Research Institute 35, 415-456.

Atwater B. F. and Belknap D. F. 1980. Tidal-wetland deposits of the Sacramento-San Joaquin Delta, California. Pacific Coast Paleogeography Symposium 4, 89-103.

Atwater B. F. 1982. Geologic maps of the Sacramento-San Joaquin Delta, California, Miscellaneous Field Studies Map MF-1401, 1:24,000 scale, U. S. Geological Survey, Reston, accessed 26 August 2020 from the National Geologic Map Database, http://ngmdb.usgs.gov/Prodesc/proddesc_7126.htm

Bullen K. E. and Bolt B. A., 1985. An introduction to the theory of seismology, 4th ed., Cambridge Univ. Press, 499 pp.

Building Seismic Safety Council 2001. 2000 Edition, NEHRP Recommended Provisions for Seismic Regulations for New Buildings and Other Structures, FEMA-368, Part 1 (Provisions): developed for the Federal Emergency Management Agency, Washington, D.C.

Craig M. and Hayashi K. 2016. Surface wave surveying for near surface site characterization in the east San Francisco Bay Area, California. Interpretation, v 4, no. 4, SQ59–SQ69, http://dx.doi.org/10.1190/INT-2015-0227.1.

California Department of Water Resources, 1958. Salinity Control Barrier Investigation. Primary Subsurface Exploration on McDonald Tract and Mildred Island. Plan and Profile of Borings.

ENGEO Inc. 2011. Log of Boring 1-B2. Geotechnical Exploration, McDonald Island Setback Levee, San Joaquin County, CA. Courtesy KSN, McDonald Island GIS Portal, accessed 1 August 2020: https://www.arcgis.com/apps/MapSeries/index.html?appid=37d32f49745945eaa188dd21259 4fe7b#

Gazetas, G., 1982, Vibrational characteristics of soil deposits with variable wave velocity, International Journal for Numerical and Analytical Methods in Geomechanics, 6, 1-20. doi: 10.1002/nag.1610060103.

Geometrics Inc. 2009. SeisImager/SW^{TM} Manual. Windows Software for Analysis of Surface Waves. Manual v. 3.0.

Hayashi K., Inazaki, T, Kitao K. and Kita, T. 2019. Statistical Estimation of Soil Parameters in from Cross-Plots of S-Wave Velocity and Resistivity Obtained by Integrated Geophysical Method. In: Levees and Dams, Advances in Geophysical Monitoring and Characterization, eds. J. Lorenzo and W. Doll, Springer, https://doi.org/10.1007/978-3-030-27367-5

Hayashi, K., Inazaki, T., Kitao, K., and Kita, T., 2013. Statistical estimation of geotechnical soil parameters in terms of cross-plots of S-wave velocity and resistivity in Japanese levees, SEG Technical Program Expanded Abstracts 2013, p. 1259-1263, https://doi.org/10.1190/segam2013-0642.1

Hayashi K. and Craig M. 2017. S-wave velocity measurement and the effect of basin geometry on site response, east San Francisco Bay area, California, USA. Physics and Chemistry of the Earth 98, 49-61, http://dx.doi.org/10.1016/j.pce.2016.07.001

Hayashi K., Craig M., Kita T. and Inazaki, T., 2015. CMP spatial autocorrelation analysis of multichannel passive surface-wave data. SEG Technical Program Expanded Abstracts 2015, 2200-2204.

Hayashi K., Lorenzo J. M., and Gostic A. 2018. Application of 2D ambient noise tomography to levee safety assessment in New Orleans. The Leading Edge, Oct. 2018, 810-815, https://doi.org/10.1190/tle37100810.1.

Hayashi K. and Suzuki H. 2004. CMP cross-correlation analysis of multi-channel surface-wave data. Exploration Geophysics 35, 7-13.

Ingebritsen S. E. and Ikehara M. E. 1999. In: Sacramento-San Joaquin Delta—The Sinking Heart of the State. Land Subsidence in the United States. U. S. Geological Survey Circular, ed. D L Galloway D. L., Jones D. R. and Ingebritsen S. E., 1182, 83–94.

Ivanov, J., Miller, R. D., Lacombe, P., Johnson, C. D., and Lane, J. W. Jr. 2006, Delineating a shallow fault zone and dipping bedrock strata using multichannel analysis of surface waves with a land streamer: Geophysics, v. 71, no. 5, p. A39-A42, https://doi.org/10.1190/1.2227521

Louie J. N. 2001. Faster, Better: Shear-Wave Velocity to 100 Meters Depth from Refraction Microtremor Arrays. Bulletin of the Seismological Society of America 91, 347-364.

Lowney Associates 2004. Exploratory Boring EB-1, Project 2053-1, McDonald Island, 6/23/04, Completion Depth 55.5 ft. Obtained from California Department of Water Resources.

Okada H. 2003. The microtremor survey method. Society of Exploration Geophysicists, Monograph Series No. 12, 150 pp.

Mount J. and Twiss R. 2005. Subsidence, Sea Level Rise, and Seismicity in the Sacramento–San Joaquin Delta. San Francisco Estuary and Watershed Science v 3, iss 1, art 5, 15 pp. http://repositories.cdlib.org/jmie/sfews/vol3/iss1/art5

Park C., Miller R. and Xia, J. 1999. Multichannel analysis of surface waves. Geophysics 64, 800-808.

Planès, T., Rittgers, J. B., Mooney, M. A., Kanning, W., and Draganov, D., 2017, Monitoring the tidal response of a sea levee with ambient seismic noise: Journal of Applied Geophysics, 138, 255-263.

Rahimi, S., Wood, C. M., Coker, F., Moody, T., Bernhardt-Barry, M., and Mofarraj Kouchaki, B., 2018, The combined use of MASW and resistivity surveys for levee assessment: A case study of the Melvin Price Reach of the Wood River Levee: Engineering Geology, 241, 11-24.

Reynolds, J. M. 2011. An introduction to applied and environmental geophysics, 2nd ed. Wiley-Blackwell. 695 pp.

Unruh, J., Hitchcock, C., Blake, K., and Hector, S. 2016. Characterization of the Southern Midland Fault in the Sacramento-San Joaquin Delta, In: Applied Geology in California, Anderson R. and Ferriz H., Association of Environmental & Engineering Geologists Special Publication 26, Star Publishing Co., Belmont CA, Chap. 39, pp. 757-775.

Wills C. J. and Clahan K. B. , 2006. Developing a map of geologically defined site-condition categories for California. Bulletin of the Seismological Society of America. 96, 1483-1501. doi: 10.1785/0120050179

Wills, C. J., Gutierrez, C. I., Perez F. G. and Branum D. M., 2015. A next generation VS30 map for California based on geology and topography. Bulletin of the Seismological Society of America, 105, 3083-3091. doi: 10.1785/0120150105

Wolff, J. 2003. Delta Primer – a field guide to the California Delta. William Stout Publishers, San Francisco, Calif. 195 pp.

Xia J., Miller R. D. and Park C. B. 1999. Estimation of near surface shear-wave velocity by inversion of Rayleigh waves. Geophysics, 64, 691–700.